RESEARCH ARTICLE

Afferent neuropeptide Y projections to the ventral tegmental area in normal-weight male Wistar rats

Myrtille C. R. Gumbs[1,2] | Anna H. Vuuregge[1] | Leslie Eggels[1,2] |

Unga A. Unmehopa[1] | Khalid Lamuadni[1] | Joram D. Mul[1,2] | Susanne E. la Fleur[1,2]

[1]Department of Endocrinology and Metabolism & Laboratory of Endocrinology, Department of Clinical Chemistry, Amsterdam Neuroscience, Amsterdam UMC, University of Amsterdam, Amsterdam, The Netherlands

[2]Metabolism and Reward Group, Netherlands Institute for Neuroscience, an Institute of the Royal Netherlands Academy of Arts and Sciences, Amsterdam, The Netherlands

Correspondence
Susanne E. la Fleur, Department of Endocrinology and Metabolism, Amsterdam UMC, University of Amsterdam, Meibergdreef 9, K2-283, 1105 AZ Amsterdam-Zuidoost, The Netherlands.
Email: s.e.lafleur@amsterdamumc.nl

Funding information
Academisch Medisch Centrum, Grant/Award Number: AMC PhD Scholarship; Nederlandse Organisatie voor Wetenschappelijk Onderzoek, Grant/Award Number: NWO-VICI grant 016.160.617

Abstract

The hypothalamic neuropeptide Y (NPY) circuitry is a key regulator of feeding behavior. NPY also acts in the mesolimbic dopaminergic circuitry, where it can increase motivational aspects of feeding behavior through effects on dopamine output in the nucleus accumbens (NAc) and on neurotransmission in the ventral tegmental area (VTA). Endogenous NPY in the NAc originates from local interneurons and afferent projections from the hypothalamic arcuate nucleus (Arc). However, the origin of endogenous NPY in the VTA is unknown. We determined, in normal-weight male Wistar rats, if the source of VTA NPY is local, and/or whether it is derived from VTA-projecting neurons. Immunocytochemistry, *in situ* hybridization and RT-qPCR were utilized, when appropriate in combination with colchicine treatment or 24 hr fasting, to assess NPY/*Npy* expression locally in the VTA. Retrograde tracing using cholera toxin beta (CTB) in the VTA, fluorescent immunocytochemistry and confocal microscopy were used to determine NPY-immunoreactive afferents to the VTA. NPY in the VTA was observed in fibers, but not following colchicine pretreatment. No NPY- or *Npy*-expressing cell bodies were observed in the VTA. Fasting for 24 hr, which increased *Npy* expression in the Arc, failed to induce *Npy* expression in the VTA. Double-labeling with CTB and NPY was observed in the Arc and in the ventrolateral medulla. Thus, VTA NPY originates from the hypothalamic Arc and the ventrolateral medulla of the brainstem in normal-weight male Wistar rats. These afferent connections link hypothalamic and brainstem processing of physiologic state to VTA-driven motivational behavior.

KEYWORDS
arcuate nucleus, neuroanatomy, neuropeptide, retrograde tracing, RRID: AB_2201528, RRID: AB_2307442, RRID: AB_2753189, ventral tegmental area, ventrolateral medulla

1 | INTRODUCTION

Neuropeptide Y (NPY) is one of the most potent orexigenic peptides. Hypothalamic arcuate nucleus (Arc) NPY neurons and their projections throughout the hypothalamus have received substantial attention with regards to the role of NPY in feeding behavior (Clark, Kalra, & Kalra, 1985; Mercer, Chee, & Colmers, 2011; Stanley, Chin, & Leibowitz, 1985). However, it is now recognized that NPY interacts with the reward-related brain circuitry to regulate motivational aspects of feeding behavior (Liu & Borgland, 2015; Pandit, la Fleur, & Adan, 2013; Quarta & Smolders, 2014).

For example, administration of NPY into the lateral ventricle of rats increases motivation to obtain food pellets (Jewett, Cleary, Levine, Schaal, & Thompson, 1995). The ventral tegmental area (VTA) and nucleus accumbens (NAc) are important components of the reward-related brain circuitry in mediating feeding-related motivational behavior (Hernandez & Hoebel, 1988; Meye & Adan, 2014; Wise, 2004). We have previously demonstrated that NPY infusion specifically into the VTA or NAc but not in the hypothalamus, increases motivation to work for sugar without affecting intake of freely available sugar (Pandit, Luijendijk, Vanderschuren, la Fleur, & Adan, 2014). In line with the effects of NPY on motivation, intracerebral and intra-NAc NPY infusions increase dopamine concentrations in the NAc (Quarta, Leslie, Carletti, Valerio, & Caberlotto, 2011; Sorensen et al., 2009). NPY also directly affects VTA dopaminergic neurotransmission via multiple pre- and postsynaptic mechanisms (Korotkova, Brown, Sergeeva, Ponomarenko, & Haas, 2006; West & Roseberry, 2017).

The effects of NPY on motivational behavior or mesolimbic neurotransmission have, however, been studied by applying exogenous NPY in the brain, and to date, no studies have investigated the role of endogenous NPY in these effects. The presence of NPY-1 and -5 receptors (NPY1R, NPY5R) in the NAc and VTA indicates that endogenous NPY can interact with the reward-related brain circuitry (Korotkova et al., 2006; Parker & Herzog, 1999). For the NAc, the origin of endogenous NPY is both local as well as from an afferent Arc projection (Chronwall et al., 1985; de Quidt & Emson, 1986; van den Heuvel et al., 2015). In contrast, the origin of endogenous NPY in the VTA is currently unknown. Studies on NPY-like immunoreactivity have demonstrated inconsistent results, reporting either the presence or absence of NPY-like immunoreactive cell bodies in the VTA (Chronwall et al., 1985; de Quidt & Emson, 1986; Everitt et al., 1984). Furthermore, no studies to date have directly analyzed VTA NPY afferent projections using a neuroanatomical tracing approach. Endogenous NPY in the VTA could thus originate from local VTA interneurons, from afferent projections, or from both.

The aim of this study was to determine the source of endogenous NPY in the VTA. In addition, we investigated whether local VTA NPY expression is influenced by the physiologic state of the animal. Many NPY neurons in the brain present neuroanatomical features of interneurons (de Quidt & Emson, 1986). Therefore, we hypothesized that the VTA would contain NPY-expressing interneurons. In addition, we hypothesized that the Arc and several brainstem nuclei would contain NPY-positive projections to the VTA, as these brain areas are known to contain NPY-immunoreactive neurons as well as to project to the VTA (Chronwall et al., 1985; de Quidt & Emson, 1986; Geisler & Zahm, 2005; Yamazoe, Shiosaka, Emson, & Tohyama, 1985). We investigated local VTA NPY/*Npy* expression using immunocytochemistry and in situ hybridization in normal-weight male Wistar rats. The effect of physiologic state on VTA *Npy* expression was measured by real time qPCR (RT-qPCR) of VTA brain punches of 24 hr-fasted and nonfasted controls. Afferent NPY VTA projections were determined following infusion of the fluorescence-conjugated retrograde tracer cholera toxin-Beta (CTB) into the VTA, using fluorescent immunocytochemistry and confocal microscopy to visualize colocalization with NPY-immunoreactive neurons. We examined brain regions that have

been described to contain NPY-expressing neurons as well as to project to the VTA. In addition, as not all Arc → VTA projecting neurons showed NPY immunoreactivity, we also assessed whether these neurons colocalized with proopiomelanocortin (POMC), the other major neuronal population in the Arc (Cone, 2005). This is the first study to systematically investigate the nature of the neuroanatomical relationship between NPY and the VTA of the reward-related brain circuitry.

2 | MATERIALS AND METHODS

2.1 | Animals

Male Wistar rats (Charles River breeding Laboratories, Sulzfeld, Germany), weighing 240–280 g at arrival, were habituated to a temperature (21–23°C) and light-controlled room (12:12 hr light/dark cycle, 07:00–19:00 lights on) of the animal facility of the Netherlands Institute of Neuroscience. Rats had ad libitum access to a container with standard high carbohydrate diet (Teklad global diet 2918; 24% protein, 58% carbohydrate, and 18% fat, 3.1 kcal/g, Envigo) and a bottle of tap water. The animal care committees of the Amsterdam UMC of the University of Amsterdam and the Netherlands Institute for Neuroscience approved all experiments according to Dutch legal ethical guidelines.

2.2 | Fluorescent immunocytochemistry

Every other VTA slice was used from colchicine-infused rats from the retrograde tracing experiment in which the tracer injection was not apparent (*N* = 4; see Retrograde tracing section below for details) or naïve rats perfused with cold saline and 4% paraformaldehyde (PFA) after i.p. injected pentobarbital (*N* = 3). Brains were postfixed for 24 hr in 4% PFA and cryoprotected in 30% sucrose/PBS, and subsequently frozen on dry ice and stored at −80°C. Cryostat sections (35 μm) were kept at −20°C in cryoprotectant (30%v/v glycerol, 30%v/v glyceraldehyde, 40%v/v 10×PBS). Arc slices were used as positive controls and tyrosine hydroxylase (TH) staining was used to visualize dopaminergic neurons in the VTA.

Free-floating sections were washed in tris–buffered saline (TBS; 50 mM Tris–Cl, 150 mM NaCl; pH 7.6) and incubated with 1:1,000 rabbit anti-NPY (Niepke 26/11/1988, RRID: AB_2753189, Netherlands Institute for Neuroscience; Buijs et al., 1989) and 1:1,000 mouse anti-tyrosine hydroxylase (#MAB318, RRID: AB_2201528, EMD Millipore Corporation, Temecula) in supermix (0.15 M NaCl, 0.05 M Tris, 0.25%w/v gelatin, 0.5% v/v Triton X-100, pH 7.6 at RT) in a humidified chamber for 1 hr at RT and overnight at 4°C. After TBS washes, sections were incubated for 1 hr at RT with 1:400 biotinylated goat anti-mouse IgG (H + L) (BA9200; Vector Laboratories, Burlingham) in supermix. After TBS washes, sections were incubated with 1:500 Alexa Fluor-647-Streptavidin (s32357, Invitrogen, Carlsbad) and 1:500 Alexa Fluor-488 donkey anti-rabbit IgG (H + L) (A21206, Invitrogen) in supermix for 1 hr at RT. After TBS washes, sections were rinsed in PBS and incubated with 1:150 Hoechst (Pure Blue nuclear staining dye 33342; Biorad Laboratories, Hercules) in 1×PBS for 15 min at RT. After TBS washing, sections were coverslipped with Mowiol (10%w/v [Mowiol 4-88; Calbiochem, Merck, Darmstadt, Germany] in 0.1 M Tris–HCl pH 8.5, 25%v/v glycerol) and stored in the dark at 4°C.

Procedures for immunocytochemistry for POMC are similar to those described for NPY staining. Briefly, slices were used from brains with tracer infused into the VTA (N = 6; same animals as for NPY retrograde tracing). In chronological order, antibodies for the different incubation steps were; 1:8,000 rabbit anti-POMC antibody (Lot. 01643-3, Cat# H-029-030, RRID: AB_2307442, Phoenix Pharmaceuticals, CA), 1:400 biotinylated anti-rabbit IgG (H + L) (BA1000; Vector Laboratories, Burlingham), 1:500 Alexa Fluor-647-Streptavidin (s32357, Invitrogen, Carlsbad), and 1:150 Hoechst (Pure Blue nuclear staining dye 33342; Biorad Laboratories, Hercules). Sections were stored as mentioned above.

2.3 | Fluorescent in situ hybridization

After 7 days in the animal facility, naïve animals were sacrificed by decapitation after $30\%CO_2/70\%O_2$ anesthesia for tissue collection (N = 6). Brains were rapidly dissected, frozen on dry ice and stored at $-80°C$. Cryostat sections (35 μm) of the Arc and VTA were mounted, air-dried (40 min at 37°C) and stored at $-80°C$.

Tissue, materials and solutions were kept in RNAse-free conditions until after the stringency washes (see below). Arc sections and every other VTA section was defrosted and fixed in 4%w/v PFA in PBS (20 min at 4°C). Sections were then pretreated with 0.25%v/v acetic anhydride in 0.1 M triethanolamine, washed in PBS and delipidated with 0.1% Triton X-100/PBS (10 min). After a PBS and 1× standard saline citrate solution (SSC) wash, sections were prehybridized for 1 hr in hybridization buffer (HB) containing 50%v/v formamide, 600 mM NaCl, 10 mM HEPES Buffer (pH 7.5), 5×Denhardt's solution, 1 mM EDTA and 200 μg/mL denatured herring sperm DNA in Ultra-pure water. Sections were hybridized overnight with HB containing 3,000 ng/mL denatured antisense NPY RNA probe (Larhammar, Ericsson, & Persson, 1987) in a humidified chamber at 55°C. Sequential stringency washes included; 5×SSC (5 min, 55°C), 2×SSC (1 min, 55°C), 0.2× SSC/50%v/v formamide (30 min, 55°C), and 0.2×SSC (5 min, RT). Immunological detection ensued with 5 min washing in buffer 1 containing 100 mM Tris, 150 mM NaCl in Ultra-pure water (pH 7.5), 1 hr incubation with 1%w/v blocking reagent (11096176001, Roche Diagnostics, Mannheim Germany) in buffer 1, 5 min washing in buffer 1, and 3 hr incubation in 1:1,000 anti-DIG-alkaline phosphatase (11093274910, Roche Diagnostics, Mannheim, Germany) in buffer 1. After washing (buffer 1; 2× 15 min; buffer 2; 100 mM Tris, 100 mM NaCl, 5 mM $MgCl_2$, in Ultra-pure water, pH 9.5; 1× 5 min), sections were developed by overnight incubation with NBT/BCIP coloring solution (337.5 μg/mL nitroblue tetrazolium, 175.4 μg/mL 5-bromo-4-chloro-3-indolyl phosphate p-toluidine salt, 240 μg/mL levimasole in buffer 2). After sequential washing (distilled water, 100% methanol, distilled water; 5 min), sections were prepared for TH detection. All following incubations were separated by TBS washes. Sections were incubated in 1:1,000 mouse anti-TH in supermix in a humidified chamber for 1 hr at RT and overnight at 4°C, for 1 hr with 1:400 biotinylated goat anti-mouse IgG (H + L) in supermix, and with 1:800/1:800 avidin/biotin complex (PK-6100, Vector Laboratories, Burlingham) in supermix for 1 hr at RT. Sections were developed with a Vector Red kit (SK-5100, Vector Laboratories, Burlingham), coverslipped and stored as mentioned above. Arc sections were used as a positive control. As previously tested with this NPY probe (van den Heuvel et al., 2014), no staining was seen in negative controls of VTA and Arc slices incubated without NPY probe.

2.4 | The effect of metabolic state on VTA NPY mRNA levels

After 7 days in the animal facility, naïve rats were fasted for 24 hr (10:00–10:00) or kept under ad libitum conditions (N = 8 per group), and decapitated after $33\%CO_2/66\%O_2$ anesthesia. Brains were rapidly dissected, frozen on dry ice and stored at $-80°C$.

Sections (250 μm) were cut on the cryostat to obtain punches of the Arc (Bregma -1.72 till -3.48 mm) and bilaterally of the VTA (Bregma -4.68 till -6.24 mm [Paxinos & Watson, 2007]). Sections were placed in RNAlater (Ambion, Waltham, MA) and punched with a 1 mm-diameter blunt needle. Punches were stored in 300 μL (Arc) or 500 μL (VTA) TriReagent. After homogenization using an Ultra Turrax homogenizer (IKA, Staufen, Germany), total RNA was isolated by a chloroform extraction followed by RNA purification using the Machery Nagel nucleospin RNA clean-up kit. RNA quality was determined using Agilent RNA nano chips, using the manufacturer's kit and instructions, and was analyzed with a Bioanalyzer (Agilent, Santa Clara). Only RIN values larger than 8.50 were included. cDNA synthesis was carried out using equal RNA input (124.44 ng; measured with Denovix DS11; Denovix, Wilmington) and the transcriptor first-strand cDNA synthesis kit with oligo d(T) primers (04897030001; Roche Molecular Biochemicals, Mannheim, Germany). Genomic DNA contamination was controlled for by cDNA synthesis reactions without reverse transcriptase.

Gene expression was measured using RT-qPCR with the SensiFAST SYBR no-rox kit (Bioline, London, UK) and Lightcycler® 480 (Roche Molecular Biochemicals); 2 μL cDNA was incubated in a final reaction volume of 10 μL reaction containing SensiFAST and 25 ng per primer (see Table 1 for primer sequences). PCR products were analyzed on a DNA agarose gel for qPCR product size.

2.5 | Retrograde tracing from the ventral tegmental area

After 7 days in the animal facility, rats (N = 22) were implanted with two cannulas; in the right VTA for the infusion of the retrograde tracer CTB conjugated to Alexa-555 (C-22843, Invitrogen, Bleiswijk, The Netherlands), and in the left lateral ventricle (LV) for the infusion of colchicine to block neuronal transport, which is required to visualize NPY cell bodies in the medial basal hypothalamus (de Quidt & Emson, 1986). Stereotaxic surgeries and infusions were performed as described previously (van den Heuvel et al., 2014). Rats were anesthetized with a mix of ketamine (80 mg/kg; Eurovet Animal Health, Bladel, The Netherlands), xylazine (8 mg/kg; Bayer Health Care, Mijdrecht, The Netherlands), and atropine (0.1 mg/kg; Pharmachemie B.V., Haarlem, The Netherlands) intraperitoneally and fixed in a stereotaxic frame. Lidocaine (AstraZeneca) was used for local analgesia of the periost. Permanent stainless steel guide cannulas were placed in the VTA (26 gauge; PlasticsOne, Bilaney Consultants GmbH, Düsseldorf, Germany) and LV (22 gauge) with coordinates A/P: -5.40 mm from Bregma, L: +2.4 mm, and V: -8.1 mm below the surface of the skull in an

TABLE 1 List of primers for RT-qPCR

Gene	NCBI reference number	Forward primer 5′–3′	Reverse primer 5′–3′
Npy	NM_012614.2	GACAATCCGGGCGAGGACGC	TCAAGCCTTGTTCTGGGGGCA
Npy1r	NM_001113357.1	TCTCATCGCTGTGGAACGTC	CCGCCAGTACCCAAATGACA
Npy5r	NM_012869.1	GCCGAAGCATAAGCTGTGGAT	TTTTCTGGAACGGCTAGGTGC
Ubiquitin-C	NM_017314.1	TCGTACCTTTCTCACCACAGTATCTAG	GAAAACTAAGACACCTCCCCATCA
HPRT	NM_012583.2	CCATCACATTGTGGCCCTCT	TATGTCCCCCGTTGACTGGT
Cyclophilin-A	NM_017101.1	TGTTCTTCGACATCACGGCT	CGTAGATGGACTTGCCACC

HPRT = hypoxanthine guanine phosphoribosyl transferase; Npy1r = neuropeptide Y receptor 1; Npy5r = neuropeptide Y receptor 5; Npy = neuropeptide Y.

angle of 10° in the frontal plane and A/P: −0.8 mm, L: +1.8 mm, and V: 4.0 mm below the surface of the brain, respectively. Cannulas were secured to the skull using three anchor screws and dental cement. Cannula's were occluded by stainless steel dummy cannula's. Immediately after surgery, rats received an analgesic subcutaneously (Carprofen, 0.5 mg/100 g body weight) and were housed individually for the rest of the experiment.

Directly after surgery and using pressure injection (Yi et al., 2006), 50-100 nL 1% CTB-Alexa555 was infused into the VTA at an infusion rate of 0.3 μL/min using a syringe infusion pump (Harvard apparatus) with a 10 μL Hamilton syringe connected to an injector (33 gauge, PlasticsOne) that extended 1 mm below the guide cannula. Ten days later, rats were anesthetized with pentobarbital and 100 μg colchicine (C9754, Sigma–Aldrich, Zwijndrecht, The Netherlands) in 5 μL 0.9% NaCL was infused in the LV at 10:00. Colchicine was infused at a rate of 1 μL/min. Both injections were confirmed by monitoring fluid movement in the tubing via a small air bubble. After completion of the infusion, the injector was left in place for 20 min to allow for diffusion and then replaced with dummy cannulas. Thirty hours after colchicine infusion, rats were deeply anesthetized with an i.p. injection of pentobarbital and perfused transcardially with cold saline followed by 4% PFA in 0.1 mol/L PBS (pH 7.6; 4°C). Brains were removed and, after 24 hr postfixation, cryoprotected in 30% sucrose in PBS at 4°C. Brains were frozen on dry ice and stored at −80°C.

A cut was made in the cortex to allow determination of the ipsi- and contralateral side of the tracer infusion. Slicing, storing and staining procedures were performed as for fluorescent immunohistochemistry above. The injection site was determined in VTA slices counterstained with anti-tyrosine hydroxylase (1:1,000 rabbit anti-TH; T8700, Sigma–Aldrich, Zwijndrecht, The Netherlands), biotinylated goat anti-rabbit IgG (H + L) (1:400, BA1000, Vector laboratories) and Alexa Fluor 647-Streptavidin (1:500, s32357, Invitrogen). Slices throughout the rostro-caudal length of the brain were stained for NPY as described above to determine colocalization with CTB (see below for details of the analysis). Slices were coverslipped and stored as written above for fluorescent immunocytochemistry.

2.6 | Antibody characterization

All primary antibodies used in this study have been extensively characterized. The specificity of anti-NPY was tested by preabsorption controls on human infundibular brain tissue (homologous to the rat Arc) and formalin-

bound porcine NPY to nitrocellulose paper, as well as by testing for cross-reactivity with several peptides formalin-fixed onto gelatin-coated nitrocellulose paper (Buijs et al., 1989; Goldstone, Unmehopa, Bloom, & Swaab, 2002; van der Beek et al., 1992; van Wamelen, Aziz, Anink, Roos, & Swaab, 2013). The specificity of anti-POMC was tested by preabsorption controls on Arc brain sections containing POMC neurons, where staining was abolished (Wittmann et al., 2017). The specificity of anti-TH was tested by Western Blot analysis of recombinant TH and of VTA protein homogenates, which showed that it recognized a single band of 56–60 kDa, and the absence of staining in midbrain-containing brain slices of animals in which dopamine neurons where specifically lesioned by 6-hydroxydopamine (Wang & Morales, 2008). We again confirmed the specificity of all primary and secondary antibodies by omitting the primary antibody in the staining procedure of Arc or VTA slices. This consistently resulted in complete absence of staining in the Arc or VTA. We additionally used Western Blotting to confirm that the POMC antibody specifically recognizes a 29 kDa protein in Arc lysates from naïve male Wistar rats, and that the TH antibody specifically recognizes a 55–60 kDa protein in VTA lysates. Finally, the staining patterns of all primary antibodies are in accordance with previous studies that characterized NPY and POMC staining in the Arc, and TH staining in the VTA (Wang & Morales, 2008; Wittmann et al., 2017). See Table 2 for a summary of the antibodies used in this study.

2.7 | Microscopy and image analyses

VTA slices stained for NPY mRNA were analyzed by light microscopy using a Zeiss Axioskop 9801 with 2.5× (n.a. 0.075) and 10× (n.a. 0.30) PlanNeoPlan Fluar objectives (Zeiss) and a color camera (EvolutionMP; QImaging). Fluorescent stained slices were analyzed using widefield fluorescent microscopy on a Zeiss Axiovert 200M with Plan-NeoFluar objectives at 2.5× (n.a. 0.075) and 5× (n.a. 0.16) magnification to investigate local NPY peptide expression, VTA slices for infusion site determination for retrograde tracing, and for a quick scan for colocalization. Fluorescence was excited with a HXP 120 V power supply Metalhalide lamp with excitation filters 365/12 nM (Hoechst) 560/40 nM (Alexa Fluor 555), 470/40 nM (Alexa Fluor 488), 605/50 nM (Alexa Fluor 647) and emission filters >397 nM, 603/75 nM, 515/30 nM, and 670/50 nM, respectively. Images were obtained with a black and white camera (ExiAqua, QImaging) and ImageProPlus software (version 6.3, Media Cybernetics). Colocalization was confirmed with confocal image series

TABLE 2　Antibodies used in this study

Antibody (dilution)	Immunizing agent	Manufacturer/Cat#/RRID/Clonality	Reference
Rabbit anti-NPY (1:1,000)	Full porcine NPY-peptide conjugated to thyroglobulin with glutaraldehyde: YPSKPDNPGEDAPAE DLARYYSALRHYINLITRQRY-NH2	Netherlands Institute for Neuroscience/ n.a./RRID: AB_2753189/polyclonal	(Buijs et al., 1989; Goldstone et al., 2002; van der Beek et al., 1992; van Wamelen et al., 2013)
Rabbit anti-POMC (1:1,000)	N-terminal 26 amino acids of porcine POMC: WCLESSQCQDLSTESNLLACIRCACKP	Phoenix Pharmaceuticals/#H-029-030/ RRID: AB_2307442/polyclonal	(Wittmann et al., 2017)
Mouse anti-TH (1:1,000)	Tyrosine hydroxylase purified from PC12 cells	EMD Millipore Corporation/#MAB318/ RRID: AB_2201528/monoclonal	(Wang & Morales, 2008)
Rabbit-anti-TH (1:1,000)	SDS-denatured rat tyrosine hydroxylase purified from pheochromocytoma	Sigma–Aldrich/#T8700/n.a./polyclonal	n.a.
Biotinylated goat anti-mouse IgG (H + L) (1:400)	Mouse IgG	Vector Laboratories/BA9200/RRID: AB_2336171/polyclonal	n.a.
Biotinylated goat anti-rabbit IgG (H + L) (1:400)	Rabbit IgG	Vector Laboratories/BA1000/RRID: AB_2313606/polyclonal	
Alexa Fluor-488 donkey anti-rabbit IgG (H + L) (1:500)	Rabbit IgG	Invitrogen/A21206/RRID: AB_2535792/polyclonal	n.a.

n.a. = not applicable.

made with a Leica TCS SP8 X confocal microscope encompassing a Z-stack of the entire slice thickness and sequential excitation with a diode for Hoechst (450 nm), and a white light laser for CTB (555 nM) and NPY (647 nM). Hybrid detection settings were 415–460 nM, 565–605 nM, and 657–700 nM, respectively. All images were taken with the same excitation and emission parameters. Image series were taken with 20× (n.a. 0.75) and 63× (n.a. 1.40) oil-immersion objectives with Immersol 518F (Zeiss) acquired at a digital resolution of 1024 × 1024 pixels in a unidirectional scan. Minimal Z-stack resolution was 2.50 μM.

For retrograde tracing, all LV cannulas were placed correctly as determined using thionine staining. Animals were included in retrograde tracing analysis when CTB and TH-fluorescence overlapped with minimal CTB outside the TH-stained area or when the CTB fluorescent pattern was comparable to Geisler and Zahm (2005), using a similar approach to map all afferent projections to the VTA. Widefield fluorescent images were analyzed with ImageJ (Rasband, http://rsbweb.nih.gov/ij/, 1997–2005) and confocal images with LAS AF Lite X (version 2.6.3, Leica microsystems). Every 10th slice was selected, stained and counted for the entire brain (Bregma 5.64 till −15.00 mm). For the Arc region (Bregma −1.08 till −4.68 mm) every 6th slice was sampled. Regions of interest were selected based on known VTA afferents from literature (Geisler & Zahm, 2005; Yetnikoff, Lavezzi, Reichard, & Zahm, 2014) and which express NPY peptide. In widefield images for investigation of colocalization, structures were delineated based on anatomical markers (visual anatomical structures such as ventricles or fiber tracts, and DAPI-staining) and NPY staining patterns. In regions where colocalization was detected, regions of interest were determined based on, and therefore always completely encompassed, the staining pattern of NPY or POMC in Z-stack confocal image series as those areas lack specific anatomical markers. Arc POMC neurons extend laterally into the peri-arcuate region, therefore POMC analysis included this area. For the brainstem region, this area was conform to the A1 and C1 catecholaminergic regions as described previously (Everitt et al.,

1984; Harfstrand, Fuxe, Terenius, & Kalia, 1987; Sawchenko & Swanson, 1982). The Arc was thus contained in 11 sections at 210 μm intervals, and the brainstem area containing colocalization was contained in 8 sections at 350 μm intervals.

In structures determined to contain colocalization (by widefield image analysis and verification by confocal microscopy), the number of labeled neurons were counted in all sections that contained the structure according to the rat brain atlas (Paxinos & Watson, 2007). Structures were counted as cells if they contained a Hoechst-stained nucleus that was completely contained in the Z-stack, showed fluorescence at least 2× above background (executed by excluding signal intensity below 2× background, which was determined in slices incubated according to the staining protocol without primary antibody), and did not show an aberrant staining pattern (e.g., red or green fluorescence in the nucleus). The abundance of NPY cells in the Arc complicated their counting. Therefore, all CTB-containing cells within the NPY-regions were counted by scrolling through the Z-stack in the red and blue channel and labeling CTB neurons according to our criteria. Subsequently, colocalization was determined in recognized CTB cells by enabling the green channel within as well as next to the red channel. CTB-positive and CTB/NPY-positive neurons were counted ipsilateral and contralateral to the CTB infusion site. As all six rats showed a consistent number of CTB and CTB/NPY-positive neurons, the data are presented as the mean of the estimated total neuron number (N), calculated using the following equation: $N = \Sigma Q^- \cdot t/h \cdot 1/asf \cdot 1/ssf$, where ΣQ^- = total number of neurons counted per region, t = thickness of the section, h = height of the section, asf = areal sampling fraction, and ssf = section sampling fraction (West, Slomianka, & Gundersen, 1991). In our study t/h is equal to 1 as the entire section thickness was included, and 1/asf also equals 1 as the entire area of the region of interest was included. Therefore, the used formula equals to $N = \Sigma Q^- \cdot 1/ssf$ with ssf = 6 for the Arc and ssf = 10 for the brainstem. Subsequently, the percentage CTB-NPY/total CTB cells was calculated per hemisphere. In all

other regions, confocal microscopy confirmed absence of colocalization. Counts were performed independently by two investigators.

2.8 | Statistics and analyses

RT-qPCR quantification was performed using LinReg Software (Ramakers, Ruijter, Deprez, & Moorman, 2003). Samples deviating >5% from the mean PCR efficiency and outliers (Grubb's test) were excluded. Factor_qPCR (version January 2016.0; Ruijter et al., 2006) was used for factor correction, and values were normalized using the geometric mean of three reference gene values (*Ubiquitin-C*, *Hypoxanthine guanine phosphoribosyl transferase* and *Cyclophilin-A*; see Table 1). All values were normalized to ad libitum controls. Compliance with normality and equal variance assumptions were confirmed with Shapiro–Wilk and Levene's test for equal variances, respectively. Differences between groups were then evaluated using Two-way ANOVA analysis followed by the Bonferroni method for multiple comparisons (IBM SPSS version 24). All data are presented as mean ± *SEM*.

3 | RESULTS

3.1 | Assessment of local NPY/*Npy* expression in the VTA

Many NPY-expressing neurons present anatomical characteristics representative of interneurons (de Quidt & Emson, 1986). Therefore, we first determined whether the VTA contains NPY-immunoreactive cell bodies using fluorescent immunocytochemistry in brain slices containing the VTA (Figure 1a). NPY-immunoreactive fibers were found scattered throughout the VTA (Figure 1b–d,h). In contrast, no NPY-immunoreactive cell bodies were found throughout the full rostro-caudal extent of the VTA. Visualization of NPY can be enhanced by pretreatment of animals with colchicine, which arrests neuronal peptide transport (Borisy & Taylor, 1967; de Quidt & Emson, 1986). Consistent with the effects of colchicine on neuronal peptide transport, no NPY-immunoreactive fibers were found in the VTA (Figure 1e–g). Furthermore, colchicine treatment did not visualize NPY-immunoreactive cell bodies throughout the VTA. Collectively,
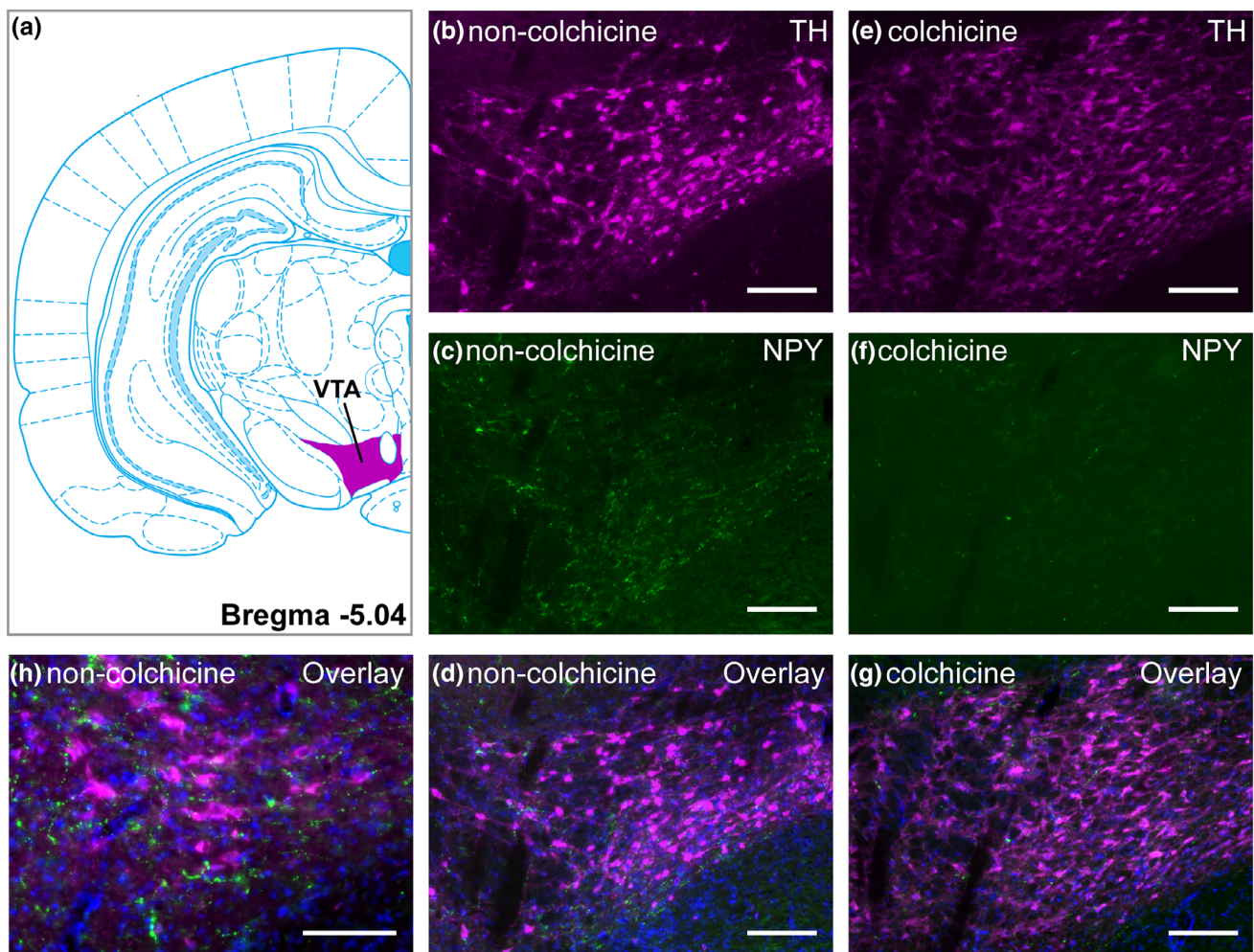

FIGURE 1 NPY-immunoreactive fibers, but not cell bodies, in the VTA. (a) Drawing of a coronal atlas section at Bregma −5.04 indicating the representative VTA area as shown in further pictures. Atlas figure adapted from Atlas figure adapted from Paxinos and Watson (2007). (b, c, d) Tyrosine hydroxylase (TH) staining, NPY staining, and an overlay with nuclear staining (Hoechst) in nontreated rats. (e, f, g) TH, NPY and an overlay staining with nuclear staining in colchicine-treated rats. (h) Overlay image showing TH, NPY, and Hoechst staining in nontreated rats at 20× magnification. b–g at 5× magnification, scale bar = 100 μm; h, scale bar = 150 μm; TH = magenta, NPY = green, Hoechst = blue [Color figure can be viewed at wileyonlinelibrary.com]

these observations indicate that the NPY-immunoreactive fibers are part of an NPY afferent projection to the VTA.

We next used in situ hybridization to confirm the absence of NPY-expressing cell bodies in the VTA. Throughout the VTA, no *Npy*-expressing cell bodies were observed (Figure 2a,b). In contrast, *Npy*-expressing cell bodies were observed in the posterior lateral hypothalamic area and the medial supramammillary nucleus (Figure 2a,c), both located adjacent to the anterior VTA. As expected, positive control slices containing the Arc also showed strong expression of *Npy* in cell bodies (Figure 2d). Taken together, these findings indicate that NPY is not locally produced in the VTA, and that NPY afferents project to the VTA.

3.2 | Modulation of *Npy* expression by physiologic state

Next, we used RT-qPCR, a sensitive method that allows the measurement of very low mRNA copy numbers (Bustin, 2000), to exclude that

VTA neurons express *Npy*. In *ad libitum*-fed normal weight male rats, *Npy* expression in VTA punches was practically negligible compared to *Npy* expression in the Arc, but not completely absent (Figure 3a).

NPY levels vary with physiological state in certain brain regions. For example, a 24 hr fast increases *Npy* expression in the Arc of the hypothalamus (Hahn, Breininger, Baskin, & Schwartz, 1998; Marks, Li, Schwartz, Porte Jr., & Baskin, 1992). We therefore determined if 24 hr fasting induces *Npy* expression locally in the VTA. See Figure 3b for the experimental setup and Figure 3c for punch areas. In accordance with previous studies (Hahn et al., 1998; Marks et al., 1992), Arc *Npy* expression was increased by ~40% after a 24 hr fast (Figure 3a; Two-way ANOVA interaction: $F_{1,22}$ = 317.9, p < .0001; post hoc Arc ad lib vs. fasting, p = .0007). In contrast, a 24 hr fast did not modulate VTA *Npy* expression, which remained practically negligible (Figure 3a; post hoc VTA ad lib vs. fasting, p > .05). We also measured expression of two NPY receptors, *Npy1r* and *Npy5r*, in the VTA. Both receptors were
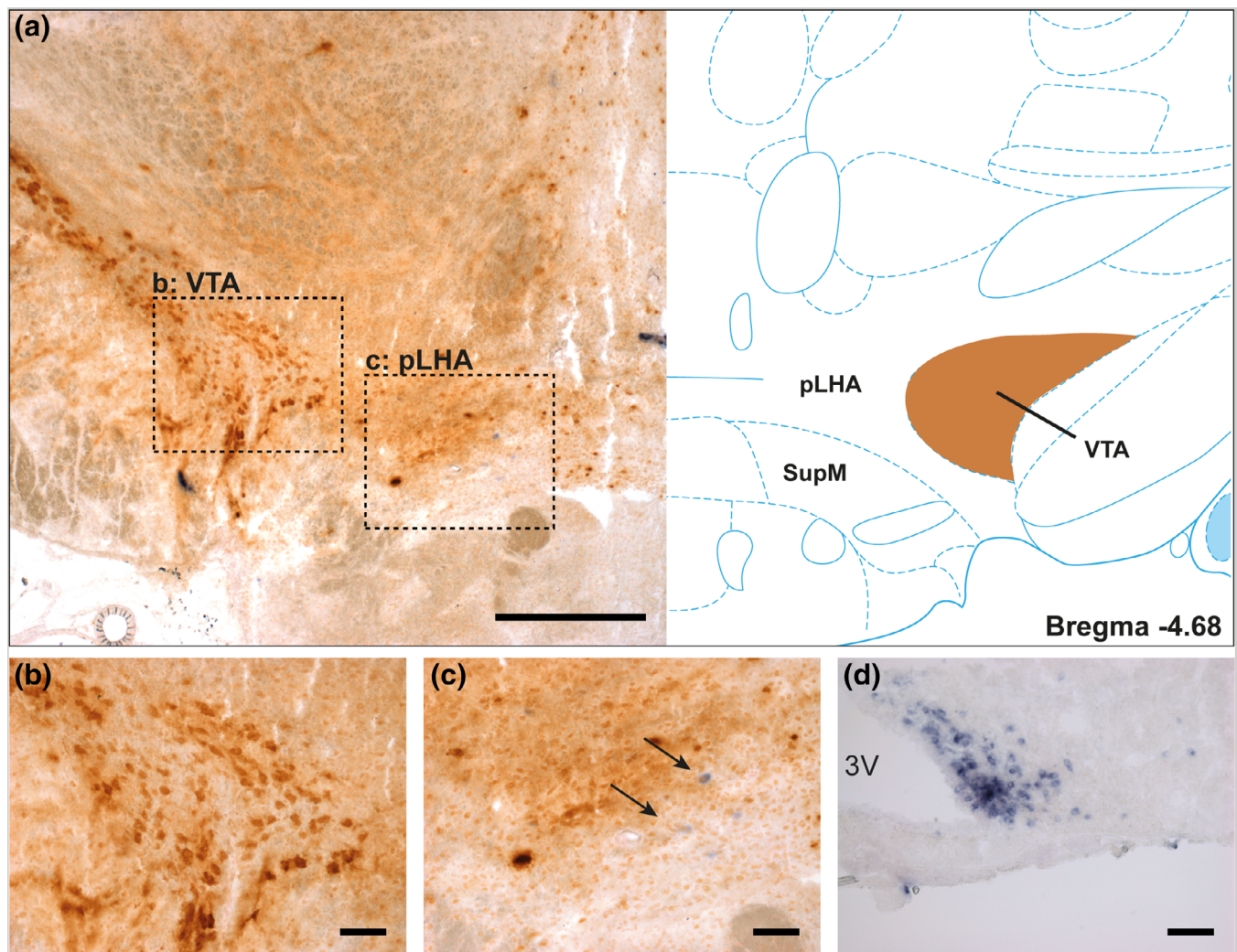
FIGURE 2 *Npy*-expressing cell bodies in the posterior lateral hypothalamic area, but not the VTA. (a, left) A coronal VTA section at Bregma −4.68 stained for *Npy* (blue) by *in situ* hybridization and tyrosine hydroxylase (TH; brown) immunocytochemistry, and (a, right) drawing of a coronal atlas section to indicate the VTA, posterior lateral hypothalamic area (pLHA), and the medial supramammillary nucleus (SupM). Atlas figure adapted from Paxinos and Watson (2007). (b) Inset of the VTA area showing TH-positive cell bodies, but absence of *Npy*-positive cell bodies. (c) Inset of the pLHA/SupM showing *Npy*-positive cell bodies, indicated by arrows. (d) A coronal Arc section showing *Npy*-positive cell bodies. a, scale bar = 500 μm; b–d, scale bar = 100 μm [Color figure can be viewed at wileyonlinelibrary.com]
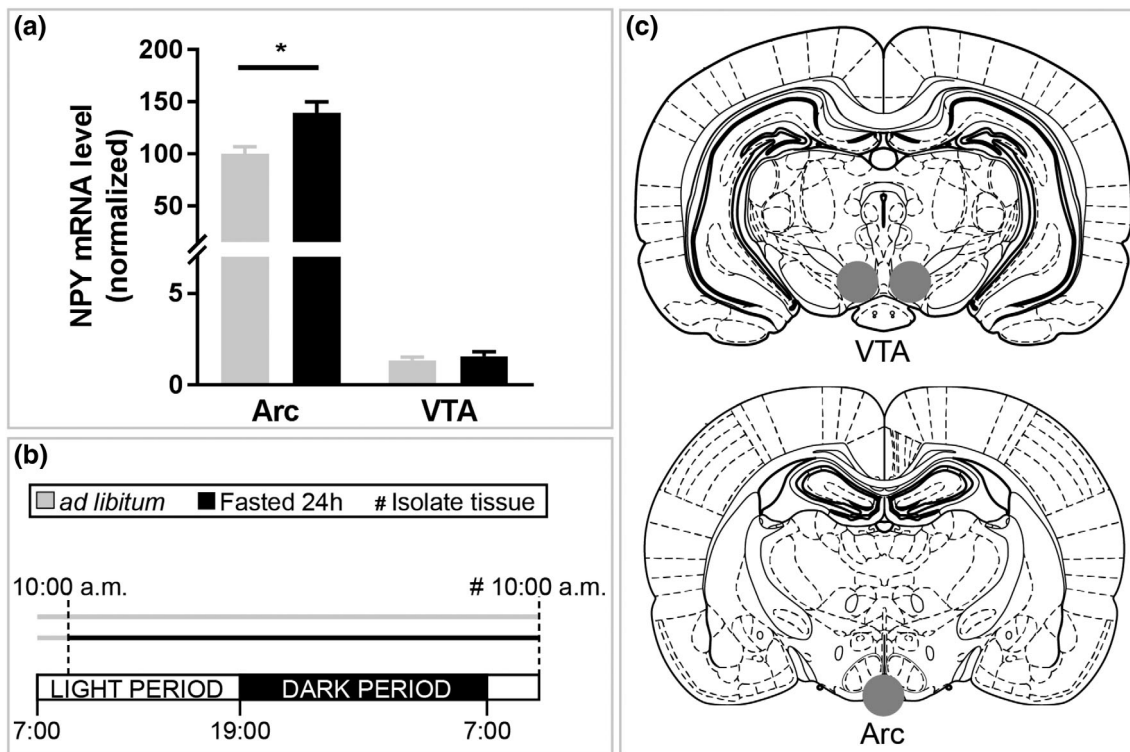
FIGURE 3 A 24 hr fast increases *Npy* expression in the Arc, but does not induce *Npy* expression in the VTA. (a) *Npy* expression in the Arc and VTA at the beginning of the light period, normalized to three reference genes and expressed as percentage of Arc ad libitum levels. *Npy* expression in the Arc was modulated by a 24 hr fast (*post hoc*; *$p < .001$). VTA *Npy* expression was barely detectable compared to Arc levels, and not modulated by a 24 hr fast (post hoc; $p > .05$). (b) Schematic overview of the experimental setup and timeline. Rats were fasted for 24 hr or fed *ad libitum* before sacrifice at the beginning of the light period. (c) Coronal rat brain drawing indicating the punch areas for the respective regions. Atlas figures adapted from Paxinos and Watson (2007). $N = 6/7$ per group

expressed in the VTA, but not regulated by a 24 hr fast (data not shown). Together with our neuroanatomical data, these observations confirm that the origin of endogenous VTA NPY comes predominantly, if not completely, from an afferent projection to the VTA.

3.3 | Identification of NPY-immunoreactive afferents to the VTA

To study the origin of NPY afferents to the VTA, we infused the retrograde tracer CTB into the VTA, followed by infusion of colchicine prior to sacrifice to enhance visualization of NPY (de Quidt & Emson, 1986). Six rats showed CTB infusions confined to the VTA region (Figure 4a–d). In these animals, whole-brain serial sections showed CTB labeling throughout the brain (Figure 5) in a pattern consistent with previously reported VTA afferents (Geisler & Zahm, 2005; Yetnikoff et al., 2014). Throughout the brain, several regions showed both NPY-immunoreactive neurons and CTB-containing neurons. We included all regions known to contain NPY neurons, to project to the VTA and to be involved in motivational or reward-related behavior (see Table 3). In all six rats, the Arc of the hypothalamus contained neurons that were double-stained with NPY and CTB (Figure 6a,b). Over all animals, a mean estimated total number of 293 ± 42 CTB-positive neurons and 64 ± 20 CTB/NPY-positive were calculated ipsilaterally to the infusion site. Contralaterally, a mean estimated total

number of 224 ± 40 CTB-positive and 57 ± 21 CTB/NPY-positive neurons were calculated. Of the CTB-positive neurons, a mean percentage of 19.8 ± 5.0% and 21.9 ± 5.8% colocalized with NPY ipsilaterally and contralaterally, respectively, throughout the entire rostro-caudal extent of the Arc. Figure 6c shows the Arc NPY region of interest schematically.

Based on known VTA projections (Geisler & Zahm, 2005; Mejias-Aponte, Drouin, & Aston-Jones, 2009) and brainstem NPY expression (Chronwall et al., 1985; de Quidt & Emson, 1986; Everitt et al., 1984; Yamazoe et al., 1985), we also expected colocalization of CTB and NPY in several brainstem structures and thus analyzed the brainstem of four CTB-infused brains (from Figure 4a–c; magenta, green, black, and orange color-coded animals were analyzed). The ventrolateral medulla showed colocalization of CTB and NPY that was limited to a region from Bregma −12.12 till −15.00 mm (Figure 7a–c). A mean estimated total number of 193 ± 64 CTB-positive neurons and 65 ± 23 CTB/NPY-positive neurons were calculated ipsilaterally. Contralaterally, a mean estimated total number of 230 ± 84 CTB-positive neurons and 28 ± 11 CTB-NPY-positive neurons were calculated. Of the CTB-positive neurons, a mean percentage of 33.8 ± 8.2% and 16.0 ± 6.2% colocalized with NPY ipsilaterally and contralaterally, respectively, in the ventrolateral medulla. Thus, the Arc as well as a part of the ventrolateral medulla of the

FIGURE 4 CTB infusion sites. (a–c) Overview of the six experimental animals with the retrograde tracer CTB confined to the VTA and used for the analysis. The region with the largest area in the coronal plane is shown at the respective Bregma level. (d) Example of CTB infusion site (magenta area in b), showing tyrosine hydroxylase (TH, green), CTB (magenta) and Hoechst (blue). Atlas figures adapted from the rat brain atlas (Paxinos & Watson, 2007). Scale bar = 500 μm [Color figure can be viewed at wileyonlinelibrary.com]
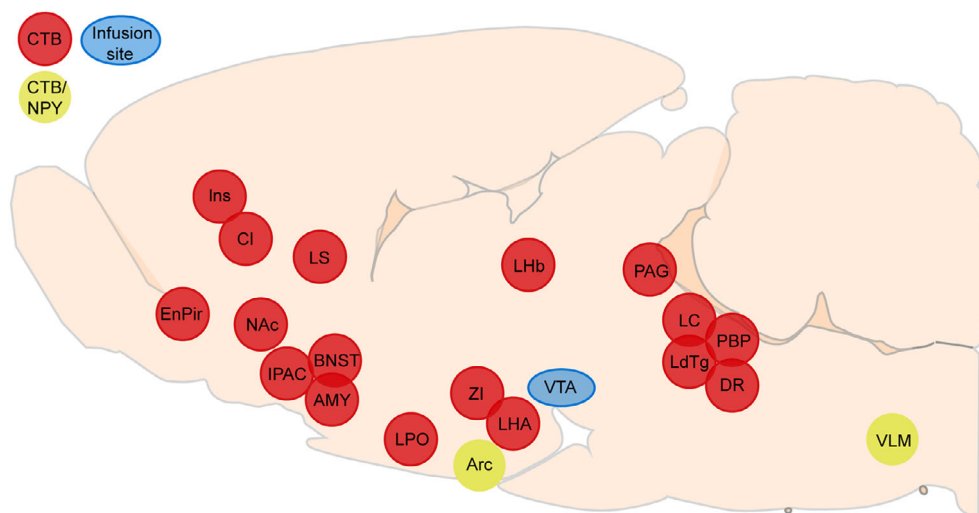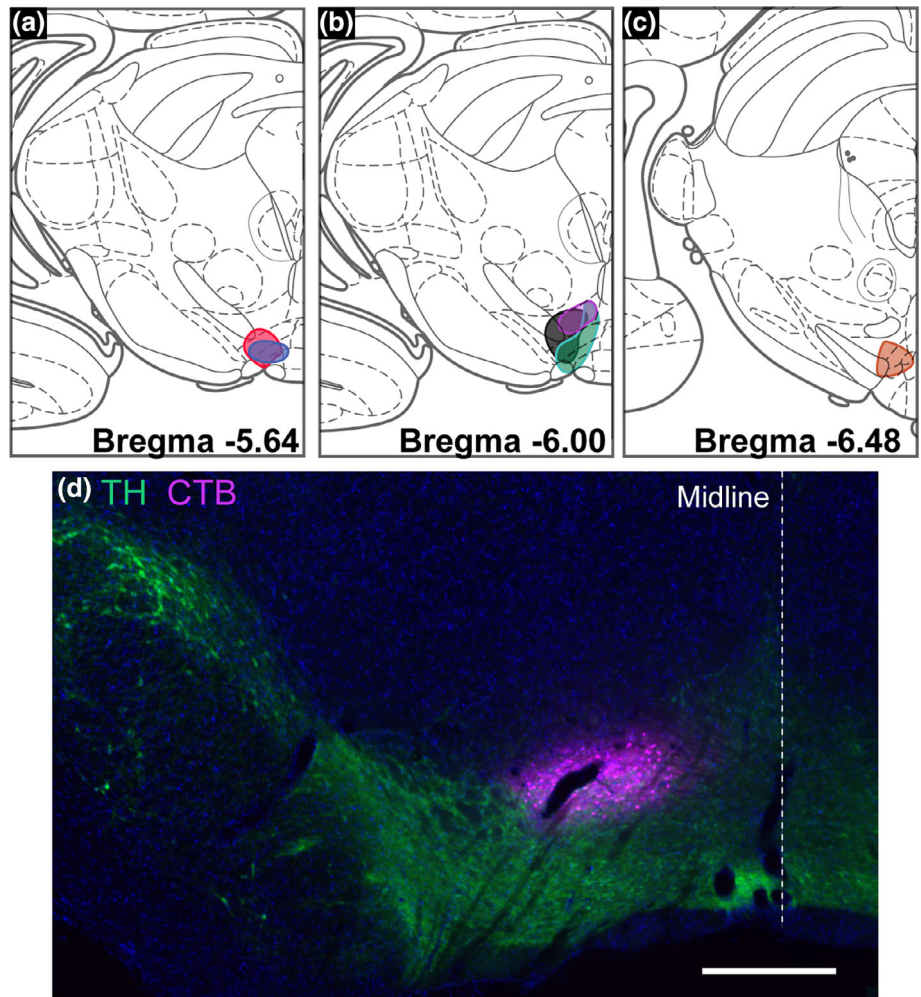

FIGURE 5 Schematic overview of identified VTA afferents using CTB. Schematic sagittal rat brain drawing showing a selection of the brain regions containing CTB neurons (red areas) following CTB infusion into the VTA (blue). The Arc of the hypothalamus and the ventrolateral medulla are the only regions showing CTB/NPY colocalization (areas indicated in yellow). Not all projections are shown for clarity. Atlas figure adapted from the rat brain atlas (Paxinos & Watson, 2007). Arc = arcuate nucleus of the hypothalamus; AMY = amygdala (all amygdala regions); BNST = bed nucleus of the stria terminalis; Cl = claustrum; DR = dorsal raphe; EnPir = endopiriform nucleus and piriform cortex; Ins = insular cortex; IPAC = interstitial nucleus of the posterior limb of the anterior commissure; LdTg = laterodorsal tegmental nucleus; LHA = lateral hypothalamic area; LHb = lateral habenula; LC = locus coeruleus; LPO = lateral preoptic area; LS = lateral septum; NAc = nucleus accumbens; PAG = periaqueductal gray; PBP = lateral and medial parabrachial nucleus; VLM = ventrolateral medulla; VTA = ventral tegmental area; ZI = zona incerta [Color figure can be viewed at wileyonlinelibrary.com]

TABLE 3 Overview of NPY-immunoreactive afferent projections to the VTA. Included regions were selected based on the current literature showing both a VTA afferent projection as well as an indication of NPY cell bodies by immunocytochemistry

VTA afferent containing NPY cell bodies	VTA projection	NPY cell bodies	Colocalization	Conclusion
Telencephalon				
Claustrum	Yes	Yes	No	Non-NPY projection
Endopiriform nucleus + piriform cortex[a]	Yes	Yes	No	Non-NPY projection
Insular cortex	Yes	Yes	No	Non-NPY projection
Nucleus accumbens (core and shell)	Yes	Yes	No	Non-NPY projection
Bed nucleus of the stria terminalis	Yes	Yes	No	Non-NPY projection
IPAC[b]	Yes	Yes	No	Non-NPY projection
Medial preoptic nucleus	Yes	Yes	No	Non-NPY projection
Ventral pallidum	Yes	Yes	No	Non-NPY projection
Amygdala[c]	Yes	Yes	No	Non-NPY projection
Lateral septum	Yes	Yes	No	Non-NPY projection
Diagonal band of Broca	Yes	No	No	Non-NPY projection
Lateral preoptic area	Yes	Yes	No	Non-NPY projection
Cingulate cortex	Yes	Yes	No	Non-NPY projection
Diencephalon				
Arcuate nucleus of the hypothalamus	Yes	Yes	Yes	NPY projection
Anterior hypothalamus	Yes	Yes	No	Non-NPY projection
Hypothalamic paraventricular nucleus	Yes	No	No	Non-NPY projection
Ventromedial hypothalamic nucleus	Yes	No	No	Non-NPY projection
Zona incerta	Yes	No	No	Non-NPY projection
Perifornical lateral hypothalamic area	Yes	No	No	Non-NPY projection
Dorsal hypothalamus	Yes	No	No	Non-NPY projection
Posterior lateral hypothalamus	Yes	Yes	No	Non-NPY projection
Mesencephalon				
Periaqueductal gray[d]	Yes	Yes	No	Non-NPY projection
Met- and Myelencephalon				
Locus coeruleus	Yes	Yes	No	Non-NPY projection
Laterodorsal tegmental nucleus	Yes	No	No	Non-NPY projection
Dorsal Raphe	Yes	No	No	Non-NPY projection
(Lateral) of Central Gray	Yes	Yes	No	Non-NPY projection
Lateral parabrachial nucleus	Yes	No	No	Non-NPY projection
Medial parabrachial nucleus	Yes	No	No	Non-NPY projection
Ventrolateral medulla	Yes	Yes	Yes	NPY projection

[a]As fluorescent immunocytochemistry does not allow the separation of the endopiriform nucleus and piriform cortex, these structures were analyzed together.

[b]IPAC = interstitial nucleus of the posterior limb of the anterior commisure.

[c]As no colocalization of NPY and CTB was found throughout all amygdala regions, these regions were analyzed together.

[d]The periaqueductal gray for the magenta case in Figure 4 contained a total of 2 CTB/NPY positive cell bodies, out of >15 CTB-positive cell bodies per brain slice containing the periaqueductal gray.

brainstem contain NPY-immunoreactive afferents projecting to the VTA in normal-weight male Wistar rats.

3.4 | Identification of POMC-immunoreactive Arc afferents to the VTA

We next investigated the identity of CTB-positive neurons in the Arc that did not express NPY. POMC-expressing neurons represent another major population of neurons in the Arc, which are a separate from the NPY population, and also project to the VTA (Hahn et al., 1998; Pandit et al., 2015). We confirmed that Arc POMC-immunoreactive neurons project to the VTA, and quantified the Arc POMC projection in the same brains used for NPY tracing (Figure 8a–c). A mean estimated total number of 592 ± 84 CTB positive neurons and 689 ± 174 CTB/NPY-positive neurons were calculated ipsilaterally to the infusion site. Contralaterally, a mean estimated total number of 134 ± 16 CTB and 142 ± 17
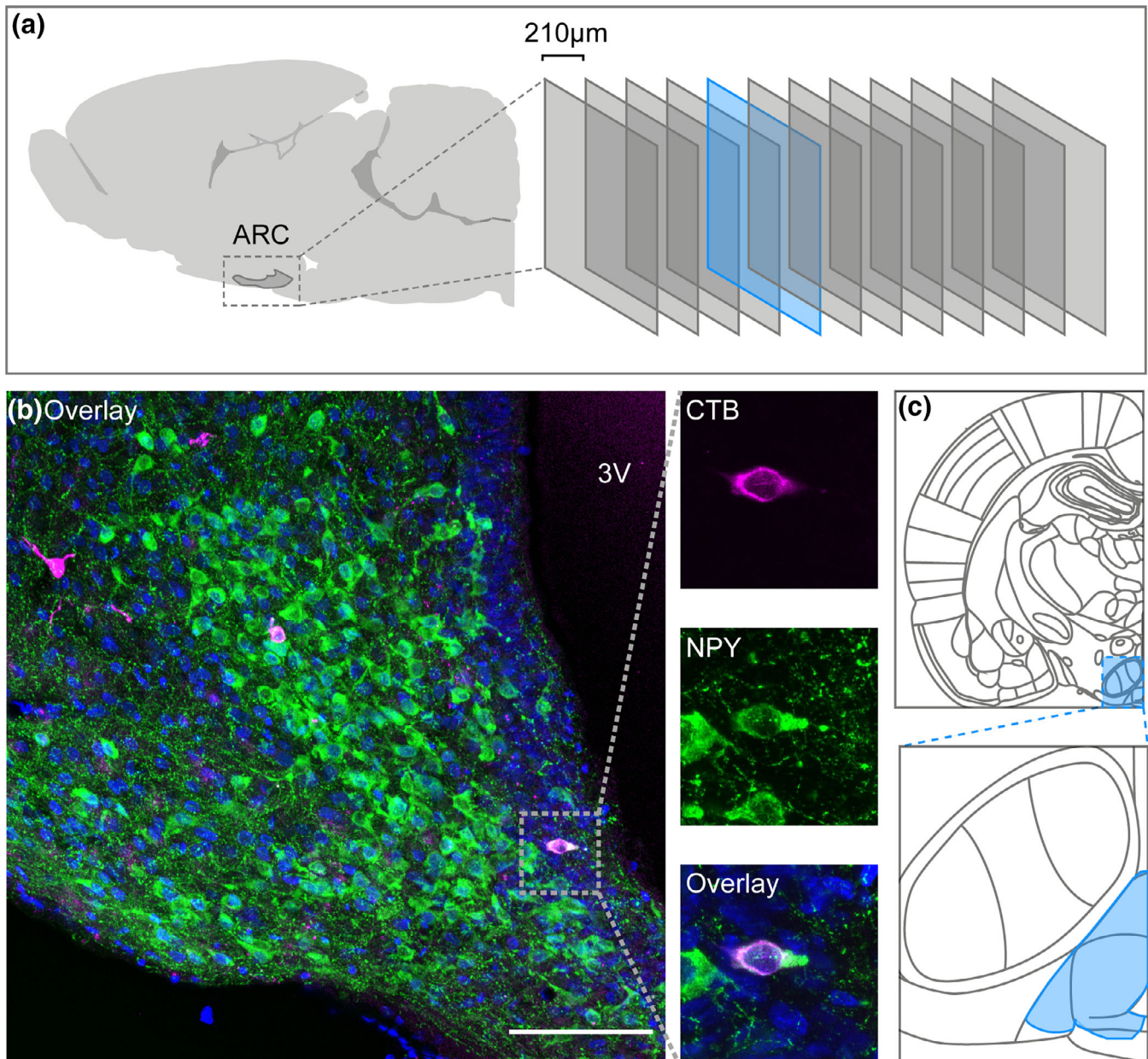
FIGURE 6 Arc NPY-immunoreactive cell bodies project to the VTA. (a) Sagittal rat brain drawing showing the location of the Arc and the slice shown in (b). (b) Randomly selected confocal fluorescent image series of a coronal Arc section showing CTB (magenta), NPY (green), Hoechst (blue), and colocalization of CTB and NPY (white). The inset is made at 63× magnification. (c) Coronal image showing the approximate region of interest for CTB cell counts in the NPY area. Atlas figures adapted from the rat brain atlas (Paxinos & Watson, 2007). Scale bar = 100 μm, 3V = third ventricle [Color figure can be viewed at wileyonlinelibrary.com]

CTB/NPY-positive neurons were calculated. The mean percentage of the CTB-positive neurons colocalizing with POMC was 21.7 ± 1.7% ipsilaterally, and 28.7 ± 4.2% contralaterally. Figure 8d shows the Arc POMC region of interest schematically.

4 | DISCUSSION

In the present study, we have characterized NPY-immunoreactive afferents projecting to the VTA. Using immunocytochemistry, we observed NPY-immunoreactive fibers, but not NPY-expressing cell bodies, in the VTA. NPY fibers in the VTA were not visible following treatment with colchicine, which arrests neuronal peptide transport. As colchicine treatment also did not lead to visualization of NPY cell bodies in the VTA and no *Npy*-expressing cell bodies were found using *in situ* hybridization, this indicates that the NPY-immunoreactive fibers come from afferent projections to the VTA. Accordingly, following infusion of the retrograde tracer CTB in the VTA, we identified cellular colocalization of CTB and NPY in the Arc of the hypothalamus and in the ventrolateral medulla of the brainstem. We did not observe
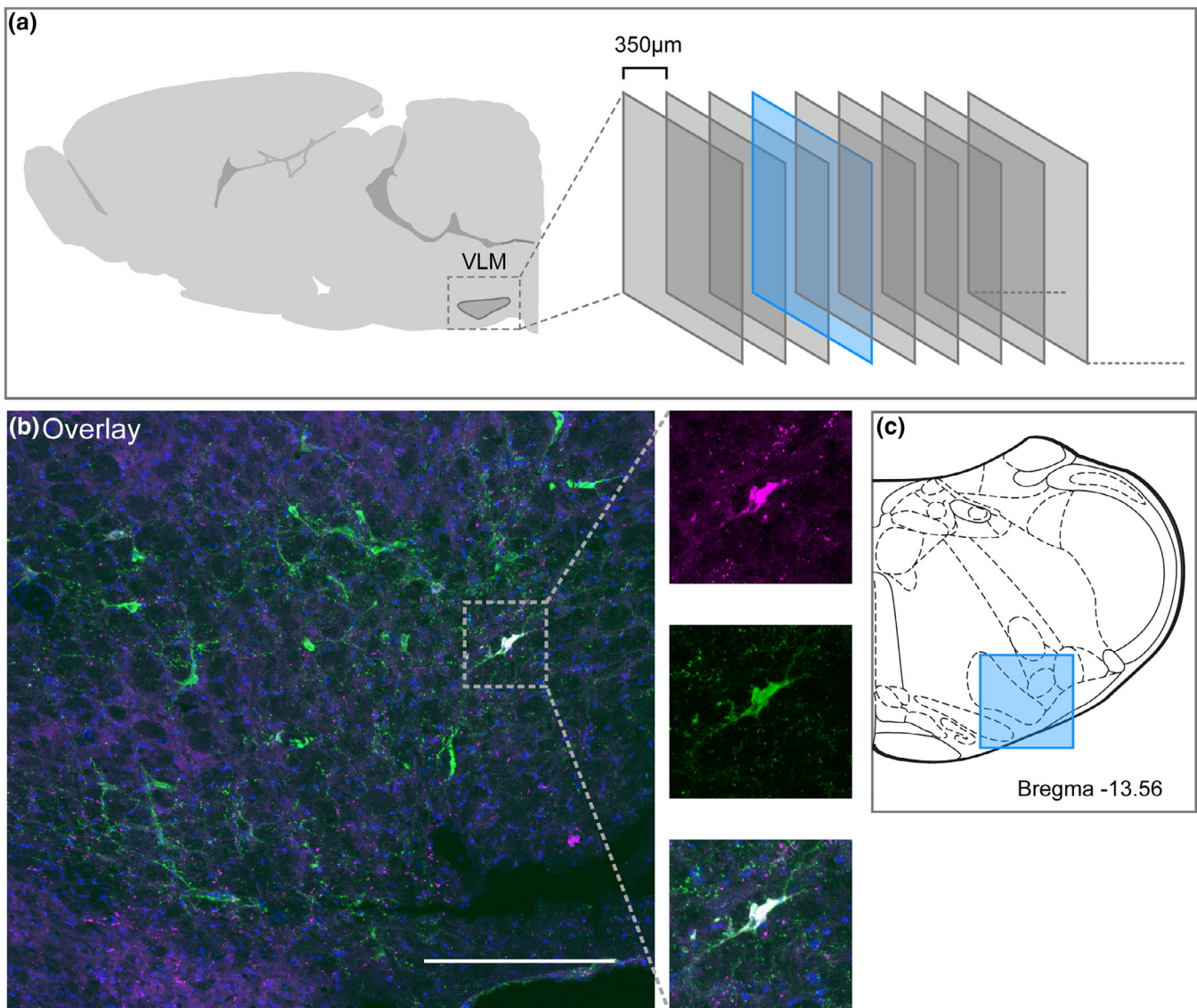
FIGURE 7 Ventrolateral medullar NPY-immunoreactive cell bodies project to the VTA. (a) Sagittal rat brain drawing showing the location of the ventrolateral medullar area and the slice shown in (b). (b) Randomly selected confocal fluorescent image series of a coronal section showing CTB (magenta), NPY (green), Hoechst (blue), and colocalization of CTB and NPY (white) and a zoom on a colocalizing cell body (magnification 20×). (c) Atlas figure showing the location of the image in (b). Atlas figures are adapted from the rat brain atlas (Paxinos & Watson, 2007). Scale bar = 250 μm [Color figure can be viewed at wileyonlinelibrary.com]

colocalization in any other brain region. To investigate if an altered metabolic state could induce *Npy* expression within the VTA, we also measured *Npy* expression following a 24 hr fast using the sensitive RT-qPCR method. However, the 24 hr fast, which was sufficient to increase *Npy* expression in the Arc, did not modulate the barely detectable levels of *Npy* expression in the VTA. Collectively, our data indicate that the Arc of the hypothalamus and the ventrolateral medulla of the brainstem are the only brain regions that contain NPY-immunoreactive afferents that project to the VTA under normal physiological circumstances.

To date, detection of NPY-immunoreactive cell bodies in the VTA has produced inconsistent results, likely driven by variation in experimental methods, such as differences in species or colchicine treatment dose and duration (Chronwall et al., 1985; de Quidt & Emson,

1986; Everitt et al., 1984). Similar to the study of de Quidt and Emson (1986), we did not observe NPY- or *Npy*-expressing cell bodies using immunocytochemistry or *in situ* hybridization, respectively. However, using RT-qPCR, a much more sensitive technique compared to *in situ* hybridization, we detected practically negligible *Npy* expression in the VTA compared to the Arc. As we identified *Npy*-expressing cell bodies in the posterior lateral hypothalamic area/medial supramammillary nucleus, located adjacent to the VTA (Figure 2a), it is likely that the very low number of *Npy* mRNA copies observed by RT-qPCR result from accidental inclusion of *Npy*-expressing cell bodies in the posterior lateral hypothalamic area/medial supramammillary nucleus in our punched VTA samples.

Despite the inconsistency in observing NPY-immunoreactive cell bodies, our study as well as all previous studies, consistently observed

FIGURE 8 POMC neurons in the Arc project to the VTA. Confocal fluorescent image series at 20× magnification showing (a) CTB (magenta), (b) POMC (green), and (c) an overlay with Hoechst (blue) in a coronal section of the Arc. (d) Coronal drawing showing the approximate region of interest for CTB cell counts in the POMC area. Atlas figures are adapted from the rat brain atlas (Paxinos & Watson, 2007). Arrows indicate colocalization. Scale bar = 100 μm. * = insets at 63×. 3V = 3rd ventricle [Color figure can be viewed at wileyonlinelibrary.com]
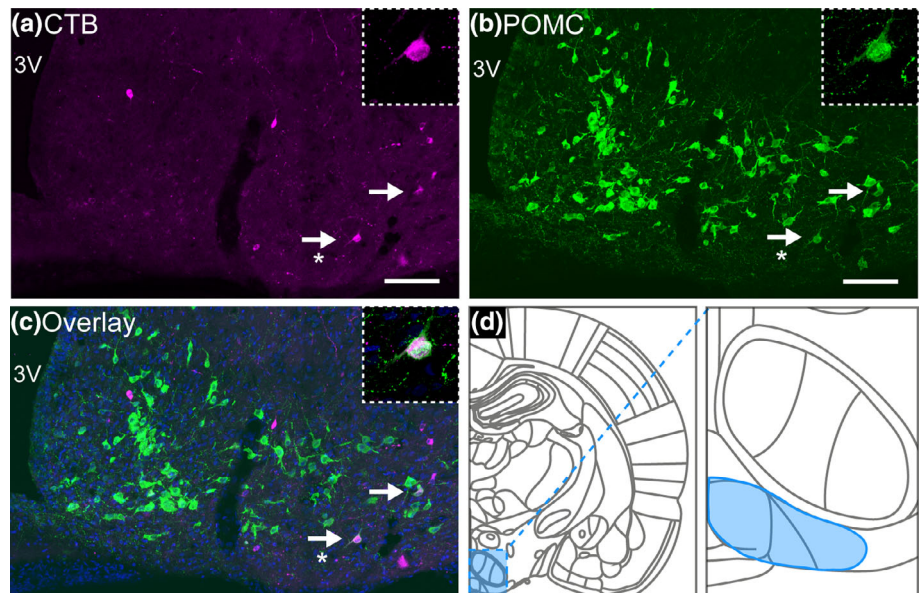
NPY-immunoreactive fibers in the VTA. In accordance with the presence of Agouti-related protein (AgRP)-immunoreactive fibers in the VTA (Broberger, Johansen, Johansson, Schalling, & Hokfelt, 1998; Dietrich et al., 2012), we found that a subset of Arc NPY-immunoreactive neurons project to the VTA. AgRP is found exclusively in the Arc, where it colocalizes almost entirely with NPY neurons (Broberger et al., 1998; Hahn et al., 1998). Although the Arc → VTA projection is considered to be relatively small compared to other VTA afferents (Geisler & Zahm, 2005; Watabe-Uchida, Zhu, Ogawa, Vamanrao, & Uchida, 2012), general activation of Arc NPY/AgRP neurons using a chemogenetic approach increases motivation to obtain food pellets, suggesting a behaviorally functional and important role for this projection in motivational and behavioral aspects of feeding behavior (Krashes, Shah, Koda, & Lowell, 2013).

We also confirm that Arc POMC neurons project to the VTA (Pandit et al., 2015). Despite a comparable percentage of VTA-projecting neurons being NPY and POMC (20–30%), it has to be noted that the absolute number of Arc CTB/POMC neurons is larger than the number of Arc CTB/NPY neurons. We believe that this difference is likely attributable to the larger POMC area in the Arc that was used for the cell counts due to the lack of visible anatomic markers for the Arc (see Section 2, Figures 6 and 8). NPY and POMC neurons are separate populations in the Arc with opposing effects on feeding behavior and energy expenditure (Aponte, Atasoy, & Sternson, 2011; Hahn et al., 1998). Future studies, utilizing chemogenetic or optogenetic manipulation of these VTA-projecting Arc NPY and POMC neuronal populations, will provide valuable insight into the role of these neurons in motivational and behavioral aspects of feeding behavior.

In addition to the NPY-immunoreactive Arc → VTA projection, we also observed colocalization of CTB and NPY in the ventrolateral medulla of the brainstem. This VTA afferent projection has previously been demonstrated using the CTB tracing approach (Geisler & Zahm, 2005), and several regions in the ventrolateral medulla contain NPY

neurons, including the A1 and C1 catecholaminergic cells groups (Everitt et al., 1984; Sawchenko et al., 1985). The population colocalizing neurons that we found is located similarly to the A1 and C1 regions. In addition, NPY neurons in the ventrolateral medulla almost completely colocalize with markers for catecholaminergic neurons (Everitt et al., 1984; Harfstrand et al., 1987; Sawchenko et al., 1985; Tseng, Lin, Wang, & Tung, 1993) and ventrolateral medulla catecholaminergic projections to the VTA were observed in male Sprague Dawley rats (Mejias-Aponte et al., 2009). Together, this might indicate that the NPYergic brainstem → VTA projection is (partially) catecholaminergic. Several studies indicate a role for catecholaminergic/NPY neurons in this area in the regulation of feeding and energy homeostasis. For example, specifically catecholaminergic/NPY neurons in the caudoventrolateral medullar area are necessary for glucoprivic feeding (Li, Wang, Dinh, & Ritter, 2009). Also, *Npy* overexpression in catecholaminergic brainstem neurons alters body composition independent of changes in food intake (Ruohonen et al., 2008; Ruohonen, Vahatalo, & Savontaus, 2012; Zhang et al., 2014). Though catecholaminergic/NPY neurons in the A1/C1 regions project to the hypothalamus (Sawchenko et al., 1985), a role for their possible connection with the VTA in regulating the above-mentioned processes cannot be excluded, and despite the relatively small size of the VTA afferent projection, it may have a substantial impact on energy homeostasis. However, additional anatomical studies will have to determine whether the NPYergic VTA projecting neurons are indeed catecholaminergic. Mechanistic studies can target the VTA-projecting NPY-expressing neurons in the ventrolateral medulla to determine their role in feeding-related motivational behaviors.

Brain area-specific NPY expression can fluctuate during increased motivation as well as hyperphagia. For example, both Arc *Npy* expression and the number of Arc NPY neurons increases during a 24 hr fast (see Figure 3b, e.g., [Hahn et al., 1998]), and hindbrain A1/C1 *Npy* expression increases during glucoprivation (Li & Ritter, 2004). Furthermore, NPY-immunoreactive cell bodies are not commonly observed in

the rat dorsomedial hypothalamus during adulthood, yet they become apparent in lactating females as well as in diet-induced obese rodents (Kesterson, Huszar, Lynch, Simerly, & Cone, 1997; Li, Chen, & Smith, 1998). In this study, we demonstrate that a 24 hr fast was not associated with increased local VTA *Npy* expression. We cannot, however, exclude that the number and/or identity of NPY-immunoreactive VTA afferents is different between sexes or during conditions with altered physiological needs, such as pregnancy and diet-induced obesity, compared to the standard physiological condition assessed in this study. In addition, infusion of colchicine in the lateral ventricle may not lead to a uniform increase in immunoreactivity in the brain, particularly in the hindbrain areas, and our tracer injection did not encompass the entire VTA, which may lead to an underestimation of the number of colocalized neurons. Lastly, the CTB tracer is not unsusceptible to uptake by fibers of passage, which could lead to the identification of a nonexistent NPY-containing VTA afferent (Chen & Aston-Jones, 1995; Ericson & Blomqvist, 1988; Luppi, Fort, & Jouvet, 1990). However, the two projections we have determined to be partially NPYergic have been described in a tracing study employing retrograde viral tracers specifically targeted to VTA dopaminergic neurons by using the Cre-Lox system (Watabe-Uchida et al., 2012). As uptake by fibers of passage is highly unlikely with this technique, we therefore believe that the assessment of NPY afferents in our study is accurate.

We demonstrate that both the Arc and a part of the ventrolateral medulla of the brainstem contain NPY-immunoreactive afferents projecting to the VTA under normal physiological circumstances in normal-weight male Wistar rats. Therefore, these brain regions link the NPY circuitry to VTA-driven changes in motivational behavior. Our study is the first to systematically investigate the origin of VTA afferent projections using neuroanatomical tracing methods. The next step will be to establish how these neuronal populations drive VTA-driven motivational behavior and whether the function of these populations is dysregulated during altered physiological states, including obesity.

DATA AVAILABILITY STATEMENT

The data that support the findings of this study are available from the corresponding author upon reasonable request.

ORCID

Myrtille C. R. Gumbs https://orcid.org/0000-0003-4347-6300

REFERENCES

Aponte, Y., Atasoy, D., & Sternson, S. M. (2011). AGRP neurons are sufficient to orchestrate feeding behavior rapidly and without training. *Nature Neuroscience*, *14*(3), 351–355. https://doi.org/10.1038/nn.2739

Borisy, G. G., & Taylor, E. W. (1967). The mechanism of action of colchicine. Binding of colchicine-3H to cellular protein. *The Journal of Cell Biology*, *34*(2), 525–533.

Broberger, C., Johansen, J., Johansson, C., Schalling, M., & Hokfelt, T. (1998). The neuropeptide Y/agouti gene-related protein (AGRP) brain circuitry in normal, anorectic, and monosodium glutamate-treated mice. *Proceedings of the National Academy of Sciences of the United States of America*, *95*(25), 15043–15048.

Buijs, R. M., Pool, C. W., Van Heerikhuize, J. J., Sluiter, A. A., Van der Sluis, P. J., Ramkema, M., … Van der Beek, E. (1989). Antibodies to small transmitter molecules and peptides: Production and application of antibodies to dopamine, serotonine, GABA, vasopressin, vasoactive intestinal peptide, neuropeptide Y, somsatostatin and substance P. *Biomedical Research*, *10*(Suppl. 3), 213–221.

Bustin, S. A. (2000). Absolute quantification of mRNA using real-time reverse transcription polymerase chain reaction assays. *Journal of Molecular Endocrinology*, *25*(2), 169–193.

Chen, S., & Aston-Jones, G. (1995). Evidence that cholera toxin B subunit (CTb) can be avidly taken up and transported by fibers of passage. *Brain Research*, *674*(1), 107–111.

Chronwall, B. M., DiMaggio, D. A., Massari, V. J., Pickel, V. M., Ruggiero, D. A., & O'Donohue, T. L. (1985). The anatomy of neuropeptide-Y-containing neurons in rat brain. *Neuroscience*, *15*(4), 1159–1181.

Clark, J. T., Kalra, P. S., & Kalra, S. P. (1985). Neuropeptide Y stimulates feeding but inhibits sexual behavior in rats. *Endocrinology*, *117*(6), 2435–2442. https://doi.org/10.1210/endo-117-6-2435

Cone, R. D. (2005). Anatomy and regulation of the central melanocortin system. *Nature Neuroscience*, *8*(5), 571–578. https://doi.org/10.1038/nn1455

de Quidt, M. E., & Emson, P. C. (1986). Distribution of neuropeptide Y-like immunoreactivity in the rat central nervous system—I. Radioimmunoassay and chromatographic characterisation. *Neuroscience*, *18*(3), 527–543.

Dietrich, M. O., Bober, J., Ferreira, J. G., Tellez, L. A., Mineur, Y. S., Souza, D. O., … Horvath, T. L. (2012). AgRP neurons regulate development of dopamine neuronal plasticity and nonfood-associated behaviors. *Nature Neuroscience*, *15*(8), 1108–1110. https://doi.org/10.1038/nn.3147

Ericson, H., & Blomqvist, A. (1988). Tracing of neuronal connections with cholera toxin subunit B: Light and electron microscopic immunohistochemistry using monoclonal antibodies. *Journal of Neuroscience Methods*, *24*(3), 225–235.

Everitt, B. J., Hokfelt, T., Terenius, L., Tatemoto, K., Mutt, V., & Goldstein, M. (1984). Differential co-existence of neuropeptide Y (NPY)-like immunoreactivity with catecholamines in the central nervous system of the rat. *Neuroscience*, *11*(2), 443–462.

Geisler, S., & Zahm, D. S. (2005). Afferents of the ventral tegmental area in the rat-anatomical substratum for integrative functions. *The Journal of Comparative Neurology*, *490*(3), 270–294. https://doi.org/10.1002/cne.20668

Goldstone, A. P., Unmehopa, U. A., Bloom, S. R., & Swaab, D. F. (2002). Hypothalamic NPY and agouti-related protein are increased in human illness but not in Prader-Willi syndrome and other obese subjects. *The Journal of Clinical Endocrinology and Metabolism*, *87*(2), 927–937. https://doi.org/10.1210/jcem.87.2.8230

Hahn, T. M., Breininger, J. F., Baskin, D. G., & Schwartz, M. W. (1998). Coexpression of Agrp and NPY in fasting-activated hypothalamic

neurons. *Nature Neuroscience*, *1*(4), 271–272. https://doi.org/10.1038/1082

Harfstrand, A., Fuxe, K., Terenius, L., & Kalia, M. (1987). Neuropeptide Y-immunoreactive perikarya and nerve terminals in the rat medulla oblongata: Relationship to cytoarchitecture and catecholaminergic cell groups. *The Journal of Comparative Neurology*, *260*(1), 20–35. https://doi.org/10.1002/cne.902600103

Hernandez, L., & Hoebel, B. G. (1988). Feeding and hypothalamic stimulation increase dopamine turnover in the accumbens. *Physiology & Behavior*, *44*(4-5), 599–606.

Jewett, D. C., Cleary, J., Levine, A. S., Schaal, D. W., & Thompson, T. (1995). Effects of neuropeptide Y, insulin, 2-deoxyglucose, and food deprivation on food-motivated behavior. *Psychopharmacology*, *120*(3), 267–271.

Kesterson, R. A., Huszar, D., Lynch, C. A., Simerly, R. B., & Cone, R. D. (1997). Induction of neuropeptide Y gene expression in the dorsal medial hypothalamic nucleus in two models of the agouti obesity syndrome. *Molecular Endocrinology*, *11*(5), 630–637. https://doi.org/10.1210/mend.11.5.9921

Korotkova, T. M., Brown, R. E., Sergeeva, O. A., Ponomarenko, A. A., & Haas, H. L. (2006). Effects of arousal- and feeding-related neuropeptides on dopaminergic and GABAergic neurons in the ventral tegmental area of the rat. *The European Journal of Neuroscience*, *23*(10), 2677–2685. https://doi.org/10.1111/j.1460-9568.2006.04792.x

Krashes, M. J., Shah, B. P., Koda, S., & Lowell, B. B. (2013). Rapid versus delayed stimulation of feeding by the endogenously released AgRP neuron mediators GABA, NPY, and AgRP. *Cell Metabolism*, *18*(4), 588–595. https://doi.org/10.1016/j.cmet.2013.09.009

Larhammar, D., Ericsson, A., & Persson, H. (1987). Structure and expression of the rat neuropeptide Y gene. *Proceedings of the National Academy of Sciences of the United States of America*, *84*(7), 2068–2072.

Li, A. J., & Ritter, S. (2004). Glucoprivation increases expression of neuropeptide Y mRNA in hindbrain neurons that innervate the hypothalamus. *The European Journal of Neuroscience*, *19*(8), 2147–2154. https://doi.org/10.1111/j.1460-9568.2004.03287.x

Li, A. J., Wang, Q., Dinh, T. T., & Ritter, S. (2009). Simultaneous silencing of Npy and Dbh expression in hindbrain A1/C1 catecholamine cells suppresses glucoprivic feeding. *The Journal of Neuroscience*, *29*(1), 280–287. https://doi.org/10.1523/JNEUROSCI.4267-08.2009

Li, C., Chen, P., & Smith, M. S. (1998). The acute suckling stimulus induces expression of neuropeptide Y (NPY) in cells in the dorsomedial hypothalamus and increases NPY expression in the arcuate nucleus. *Endocrinology*, *139*(4), 1645–1652. https://doi.org/10.1210/endo.139.4.5905

Liu, S., & Borgland, S. L. (2015). Regulation of the mesolimbic dopamine circuit by feeding peptides. *Neuroscience*, *289*, 19–42. https://doi.org/10.1016/j.neuroscience.2014.12.046

Luppi, P. H., Fort, P., & Jouvet, M. (1990). Iontophoretic application of unconjugated cholera toxin B subunit (CTb) combined with immunohistochemistry of neurochemical substances: A method for transmitter identification of retrogradely labeled neurons. *Brain Research*, *534*(1–2), 209–224.

Marks, J. L., Li, M., Schwartz, M., Porte, D., Jr., & Baskin, D. G. (1992). Effect of fasting on regional levels of neuropeptide Y mRNA and insulin receptors in the rat hypothalamus: An autoradiographic study. *Molecular and Cellular Neurosciences*, *3*(3), 199–205.

Mejias-Aponte, C. A., Drouin, C., & Aston-Jones, G. (2009). Adrenergic and noradrenergic innervation of the midbrain ventral tegmental area and retrorubral field: Prominent inputs from medullary homeostatic centers. *The Journal of Neuroscience*, *29*(11), 3613–3626. https://doi.org/10.1523/JNEUROSCI.4632-08.2009

Mercer, R. E., Chee, M. J., & Colmers, W. F. (2011). The role of NPY in hypothalamic mediated food intake. *Frontiers in Neuroendocrinology*, *32*(4), 398–415. https://doi.org/10.1016/j.yfrne.2011.06.001

Meye, F. J., & Adan, R. A. (2014). Feelings about food: The ventral tegmental area in food reward and emotional eating. *Trends in Pharmacological Sciences*, *35*(1), 31–40. https://doi.org/10.1016/j.tips.2013.11.003

Pandit, R., la Fleur, S. E., & Adan, R. A. (2013). The role of melanocortins and neuropeptide Y in food reward. *European Journal of Pharmacology*, *719*(1–3), 208–214. https://doi.org/10.1016/j.ejphar.2013.04.059

Pandit, R., Luijendijk, M. C., Vanderschuren, L. J., la Fleur, S. E., & Adan, R. A. (2014). Limbic substrates of the effects of neuropeptide Y on intake of and motivation for palatable food. *Obesity (Silver Spring)*, *22*(5), 1216–1219. https://doi.org/10.1002/oby.20718

Pandit, R., van der Zwaal, E. M., Luijendijk, M. C., Brans, M. A., van Rozen, A. J., Oude Ophuis, R. J., ... la Fleur, S. E. (2015). Central melanocortins regulate the motivation for sucrose reward. *PLoS One*, *10*(3), e0121768. https://doi.org/10.1371/journal.pone.0121768

Parker, R. M., & Herzog, H. (1999). Regional distribution of Y-receptor subtype mRNAs in rat brain. *The European Journal of Neuroscience*, *11*(4), 1431–1448.

Paxinos, G., & Watson, C. (2007). *The rat brain in stereotaxic coordinates (version 6th)*. London: Elsevier.

Quarta, D., Leslie, C. P., Carletti, R., Valerio, E., & Caberlotto, L. (2011). Central administration of NPY or an NPY-Y5 selective agonist increase in vivo extracellular monoamine levels in mesocorticolimbic projecting areas. *Neuropharmacology*, *60*(2–3), 328–335. https://doi.org/10.1016/j.neuropharm.2010.09.016

Quarta, D., & Smolders, I. (2014). Rewarding, reinforcing and incentive salient events involve orexigenic hypothalamic neuropeptides regulating mesolimbic dopaminergic neurotransmission. *European Journal of Pharmaceutical Sciences*, *57*, 2–10. https://doi.org/10.1016/j.ejps.2014.01.008

Ramakers, C., Ruijter, J. M., Deprez, R. H., & Moorman, A. F. (2003). Assumption-free analysis of quantitative real-time polymerase chain reaction (PCR) data. *Neuroscience Letters*, *339*(1), 62–66.

Ruijter, J. M., Thygesen, H. H., Schoneveld, O. J., Das, A. T., Berkhout, B., & Lamers, W. H. (2006). Factor correction as a tool to eliminate between-session variation in replicate experiments: Application to molecular biology and retrovirology. *Retrovirology*, *3*(2), 2. https://doi.org/10.1186/1742-4690-3-2

Ruohonen, S. T., Pesonen, U., Moritz, N., Kaipio, K., Roytta, M., Koulu, M., & Savontaus, E. (2008). Transgenic mice overexpressing neuropeptide Y in noradrenergic neurons: A novel model of increased adiposity and impaired glucose tolerance. *Diabetes*, *57*(6), 1517–1525. https://doi.org/10.2337/db07-0722

Ruohonen, S. T., Vahatalo, L. H., & Savontaus, E. (2012). Diet-induced obesity in mice overexpressing neuropeptide y in noradrenergic neurons. *International Journal of Peptide*, *2012*, 452524–452510. https://doi.org/10.1155/2012/452524

Sawchenko, P. E., & Swanson, L. W. (1982). The organization of noradrenergic pathways from the brainstem to the paraventricular and supraoptic nuclei in the rat. *Brain Research*, *257*(3), 275–325.

Sawchenko, P. E., Swanson, L. W., Grzanna, R., Howe, P. R., Bloom, S. R., & Polak, J. M. (1985). Colocalization of neuropeptide Y immunoreactivity in brainstem catecholaminergic neurons that project to the paraventricular nucleus of the hypothalamus. *The Journal of Comparative Neurology*, *241*(2), 138–153. https://doi.org/10.1002/cne.902410203

Sorensen, G., Wegener, G., Hasselstrom, J., Hansen, T. V., Wortwein, G., Fink-Jensen, A., & Woldbye, D. P. (2009). Neuropeptide Y infusion into the shell region of the rat nucleus accumbens increases extracellular levels of dopamine. *Neuroreport*, *20*(11), 1023–1026.

Stanley, B. G., Chin, A. S., & Leibowitz, S. F. (1985). Feeding and drinking elicited by central injection of neuropeptide Y: Evidence for a hypothalamic site(s) of action. *Brain Research Bulletin*, *14*(6), 521–524.

Tseng, C. J., Lin, H. C., Wang, S. D., & Tung, C. S. (1993). Immunohistochemical study of catecholamine enzymes and neuropeptide Y (NPY) in the rostral ventrolateral medulla and bulbospinal projection. *The*

Journal of Comparative Neurology, *334*(2), 294–303. https://doi.org/10.1002/cne.903340210

van den Heuvel, J. K., Eggels, L., Fliers, E., Kalsbeek, A., Adan, R. A., & la Fleur, S. E. (2014). Differential modulation of arcuate nucleus and mesolimbic gene expression levels by central leptin in rats on short-term high-fat high-sugar diet. *PLoS One*, *9*(1), e87729. https://doi.org/10.1371/journal.pone.0087729

van den Heuvel, J. K., Furman, K., Gumbs, M. C., Eggels, L., Opland, D. M., Land, B. B., ... la Fleur, S. E. (2015). Neuropeptide Y activity in the nucleus accumbens modulates feeding behavior and neuronal activity. *Biological Psychiatry*, *77*(7), 633–641. https://doi.org/10.1016/j.biopsych.2014.06.008

van der Beek, E. M., Pool, C. W., van Eerdenburg, F. J., Sluiter, A. A., van der Donk, H. A., van den Hurk, R., & Wiegant, V. M. (1992). Fc-mediated nonspecific staining of the porcine brain with rabbit antisera in immunocytochemistry is prevented by pre-incubation of the sera with proteins A and G. *The Journal of Histochemistry and Cytochemistry*, *40*(11), 1731–1739. https://doi.org/10.1177/40.11.1385516

van Wamelen, D. J., Aziz, N. A., Anink, J. J., Roos, R. A., & Swaab, D. F. (2013). Neuropeptide alterations in the infundibular nucleus of Huntington's disease patients. *Journal of Neuroendocrinology*, *25*(2), 198–205. https://doi.org/10.1111/j.1365-2826.2012.02379.x

Wang, H. L., & Morales, M. (2008). Corticotropin-releasing factor binding protein within the ventral tegmental area is expressed in a subset of dopaminergic neurons. *The Journal of Comparative Neurology*, *509*(3), 302–318. https://doi.org/10.1002/cne.21751

Watabe-Uchida, M., Zhu, L., Ogawa, S. K., Vamanrao, A., & Uchida, N. (2012). Whole-brain mapping of direct inputs to midbrain dopamine neurons. *Neuron*, *74*(5), 858–873. https://doi.org/10.1016/j.neuron.2012.03.017

West, K. S., & Roseberry, A. G. (2017). Neuropeptide-Y alters VTA dopamine neuron activity through both pre- and postsynaptic mechanisms. *Journal of Neurophysiology*, *118*(1), 625–633. https://doi.org/10.1152/jn.00879.2016

West, M. J., Slomianka, L., & Gundersen, H. J. (1991). Unbiased stereological estimation of the total number of neurons in thesubdivisions of the rat hippocampus using the optical fractionator. *The Anatomical Record*, *231*(4), 482–497. https://doi.org/10.1002/ar.1092310411

Wise, R. A. (2004). Dopamine, learning and motivation. *Nature Reviews. Neuroscience*, *5*(6), 483–494. https://doi.org/10.1038/nrn1406

Wittmann, G., Farkas, E., Szilvasy-Szabo, A., Gereben, B., Fekete, C., & Lechan, R. M. (2017). Variable proopiomelanocortin expression in tanycytes of the adult rat hypothalamus and pituitary stalk. *The Journal of Comparative Neurology*, *525*(3), 411–441. https://doi.org/10.1002/cne.24090

Yamazoe, M., Shiosaka, S., Emson, P. C., & Tohyama, M. (1985). Distribution of neuropeptide Y in the lower brainstem: An immunohistochemical analysis. *Brain Research*, *335*(1), 109–120.

Yetnikoff, L., Lavezzi, H. N., Reichard, R. A., & Zahm, D. S. (2014). An update on the connections of the ventral mesencephalic dopaminergic complex. *Neuroscience*, *282*, 23–48. https://doi.org/10.1016/j.neuroscience.2014.04.010

Yi, C. X., van der Vliet, J., Dai, J., Yin, G., Ru, L., & Buijs, R. M. (2006). Ventromedial arcuate nucleus communicates peripheral metabolic information to the suprachiasmatic nucleus. *Endocrinology*, *147*(1), 283–294. https://doi.org/10.1210/en.2005-1051

Zhang, L., Lee, I. C., Enriquez, R. F., Lau, J., Vahatalo, L. H., Baldock, P. A., ... Herzog, H. (2014). Stress- and diet-induced fat gain is controlled by NPY in catecholaminergic neurons. *Molecular Metabolism*, *3*(5), 581–591. https://doi.org/10.1016/j.molmet.2014.05.001